JGR Biogeosciences

RESEARCH ARTICLE
10.1029/2022JG007217

The Rate of Canopy Development Modulates the Link Between the Timing of Spring Leaf Emergence and Summer Moisture

Sander O. Denham[1], Mallory L. Barnes[1], Qing Chang[1], Mitchell Korolev[1], Jeffery D. Wood[2], A. Christopher Oishi[3], Kathryn O. Shay[1], Paul C. Stoy[4], Jiquan Chen[5], and Kimberly A. Novick[1]

[1]O'Neill School of Public and Environmental Affairs, Indiana University - Bloomington, Bloomington, IN, USA, [2]School of Natural Resources, University of Missouri, Columbia, MO, USA, [3]USDA Forest Service, Southern Research Station, Coweeta Hydrologic Laboratory, Otto, NC, USA, [4]Department of Biological Systems Engineering, University of Wisconsin – Madison, Madison, WI, USA, [5]Department of Geography, Environment, and Spatial Sciences, Michigan State University, Lansing, MI, USA

Abstract Shifts in phenological timing have important implications for ecosystem processes, with spring leaf emergence as a dominant control of carbon, water, and energy cycling. Phenological events are predominantly determined by weather and climate, therefore dynamic in time and sensitive to climate feedbacks. Improving our understanding of how ecosystems respond to changes in phenological timing will enhance our ability to assess summer soil water availability, since the timing of spring leaf emergence may lead to soil moisture deficits later in the growing season. We leveraged data from five AmeriFlux towers in central and eastern United States to investigate the extent spring leaf emergence (i.e., start of spring, *SoS*) influences rates at which forest canopies develop and how this impacts summer soil moisture (θ_{JJA}) variability. Our results indicate that ecosystem processes, specifically gross primary production (*GPP*) and evapotranspiration (*ET*), exhibit compensatory responses to varying leaf emergence; with delayed spring-onset, the canopy developed more quickly, resulting in rapid *GPP* and *ET* increases, consistent across sites. Nonetheless, early *SoS* is a relatively good indicator for potential summer soil water deficits, particularly when it occurs together with meteorological conditions (i.e., lower-than-average precipitation, hot summer temperatures) that contribute to soil water deficits. When these meteorological conditions coincide with early *SoS*, θ_{JJA} deficits are exacerbated. To the extent that these extreme conditions occur more frequently under future climate scenarios, the dynamics of spring phenology and hydroclimate may play an increasingly important role in portending the likelihood of summer water deficits, which are projected to become more severe.

Plain Language Summary Warmer spring have been occurring over the past several decades resulting in tree leaves emerging earlier in the year. As leaves emerge, transpiration is initiated transporting water that is stored in the soil back to the atmosphere. As transpiration continues to increase with increasing vegetation, more stored water is removed from the ground, and depending upon the frequency and magnitude of precipitation events to replenish this water, the potential for soil water deficits increases, possibly making an early start of spring (*SoS*) an indicator for summer soil water plant stress. However, the rate of development of forest canopies changes depending on when the leaves emerge such that an early *SoS* is characterized by more gradual canopy development whereas a later *SoS* is characterized by more rapid canopy development. The adjustment in rates of canopy development helps modulate the soil water status and ultimately how slow or how quickly the canopy develops exerts control over the time it takes the ecosystem to achieve maximum evapotranspiration.

Key Points:

- Ecosystem scale gross primary production (*GPP*) and evapotranspiration (*ET*) increase more rapidly when the start of spring occurs later
- The ratio of spring *ET* to spring potential *ET* (*ET:PET*) is higher when the spring begins earlier in the year
- Higher spring *ET:PET* can exacerbate summer soil moisture deficits, resulting in tree water stress

Supporting Information:

Supporting Information may be found in the online version of this article.

Correspondence to:

S. O. Denham,
sodenham@iu.edu

Citation:

Denham, S. O., Barnes, M. L., Chang, Q., Korolev, M., Wood, J. D., Oishi, A. C., et al. (2023). The rate of canopy development modulates the link between the timing of spring leaf emergence and summer moisture. *Journal of Geophysical Research: Biogeosciences*, *128*, e2022JG007217. https://doi.org/10.1029/2022JG007217

Received 30 SEP 2022
Accepted 23 MAR 2023

Author Contributions:

Formal analysis: Mitchell Korolev
Methodology: Kathryn O. Shay
Visualization: Mitchell Korolev

1. Introduction

Phenology is a key control on forest function and a clear bio-indicator for global change (Cleland et al., 2007; Richardson et al., 2013). The timing of plant phenological events such as spring leaf emergence and autumn leaf senescence, which are largely determined by interannual climate variability, exert strong control over ecosystem processes including carbon (C) and water cycling (Piao et al., 2007; Richardson et al., 2013). Plant phenology also controls land-surface characteristics such as albedo (Hollinger et al., 2010), canopy conductance and roughness (Blanken & Black, 2004), and microclimate (Richardson & O'Keefe, 2009; Schwartz & Karl, 1990). These surface characteristics regulate local energy cycling, thus playing a major role in mediating vegetation—climate

feedbacks (Peñuelas et al., 2009). It is broadly accepted that future warming is likely to speed up plant developmental processes and advance spring phenology in temperate forests (Polgar & Primack, 2011). However, the collective role of other environmental cues in shaping the timing and pace of canopy development is still not fully understood (Fu et al., 2015). Resolving how phenological timing, temperature, and rate of canopy development interact to determine the seasonal trajectory of carbon uptake and plant water use is essential for understanding how climate-driven shifts in phenology and meteorology will influence ecosystem function.

Earlier canopy development in spring, combined with potential delays in autumn senescence, will generally increase gross primary production (*GPP*) because the canopy is undergoing photosynthesis for a longer portion of the year. However, predictions for C cycle impacts of shifting phenology must also consider the potential for ecohydrological feedbacks driven by phenological control on evapotranspiration (*ET*). In closed, dense canopies, *ET* is driven by the interception of precipitation (*P*) and its subsequent evaporation from leaf surfaces, and transpiration (the process of water being transported from the soil back to the atmosphere via plant tissues, Oishi et al., 2010). Both transpiration (T_r) and interception are heavily influenced by phenological timing and total canopy leaf area (leaf area index, *LAI*). Longer green periods in spring and fall can increase both T_r and the amount of *P* that is intercepted and evaporated by the canopy (Helvey & Patric, 1965). Since soil moisture (θ) is dependent upon water retention within the soil matrix, which relies on inputs of water (i.e., *P*) and outputs of water (i.e., *ET*, runoff, etc.), *LAI* indirectly affects soil water availability. Therefore, increased spring T_r and interception due to early leaf emergence work in concert to reduce the amount of water available in the soil for plant use and runoff into streams (Kim et al., 2018). Consequently, enhanced springtime *ET* can lead to reductions in soil moisture which may limit C uptake in late summer and autumn (Buermann et al., 2018; Lian et al., 2020). On the other hand, increased carbon uptake when spring arrives early may dampen the impact of subsequent dry downs on annual C uptake (Grossiord et al., 2022). For example, Roman et al. (2015) showed that an early start to spring substantially mediated the negative impacts of the extreme 2012 flash drought on fluxes in the long-running Morgan-Monroe State Forest AmeriFlux site.

After spring leaf emergence (i.e., budburst) the magnitude of ecosystem C and water fluxes steadily increase over several weeks as leaves mature (Goulden et al., 1996). In the Northern hemisphere, leaf expansion evolves more quickly in years with a later start to spring leaf emergence (Klosterman et al., 2018) which likely affects the seasonality of C and water cycling. The rate at which *ET* increases following spring leaf emergence can influence water available to plants later in the growing season, though this is dependent on other abiotic factors (i.e., temperature, *P*). Leaf area expansion, much like leaf emergence, is largely dependent upon climatic factors (e.g., temperature); thus, once conditions become optimal for leaf emergence, they also quickly become advantageous for rapid leaf growth. If the rate of leaf area expansion, and therefore acceleration to *ET* maxima, is much greater when leaves emerge later in the year, then the overall effect of phenological variability on soil water regimes will likely be limited.

Here, we investigated the influence of the timing of leaf emergence in the spring, and the subsequent rate of leaf expansion to full canopy development, on summer plant water stress. Using potential evapotranspiration (*PET*) as a hydroclimatic indicator of potential water demand, we evaluated the ratio of spring *ET* to spring *PET* and its relation to growing season soil moisture (θ_{JJA}). The ratio *ET:PET* describes the extent to which actual ecosystem water use is coupled to the climate-driven potential and is thus a useful metric for disentangling the impact of shifting phenology from variability meteorology on spring water use.

We hypothesize that in years when leaves emerge earlier (i.e., earlier start of spring, *SoS*), the observed spring *ET:PET* will be greater than in years with later leaf emergence. Further, we expect the rate of canopy development to control the impact of increasing spring *ET* on growing season soil moisture dynamics. We present three possible scenarios (Figure 1) for the relationship between *SoS* and elapsed time from *SoS* to full canopy development, considering how these scenarios will affect soil moisture and *ET* dynamics. Scenario 1 illustrates that the rate of canopy development does not depend on when the season begins. Scenario 2 illustrates a scenario where the rate of canopy development occurs more *rapidly* when seasons begins *earlier;* this scenario would suggest that climate conditions are immediately optimal for rapid growth which would also result in high and sustained rates of *ET* and *PET* early and throughout the season. Finally, scenario 3 is the case in which the rate of canopy development occurs more *rapidly* when spring begins *later*, reflecting the fact that temperatures are generally warmer and more favorable for growth earlier in the year. Under scenarios 1 and 2, early leaf emergence increases spring *ET*, enhancing early season depletion of soil water as trees extract water from the soil. This effect is more

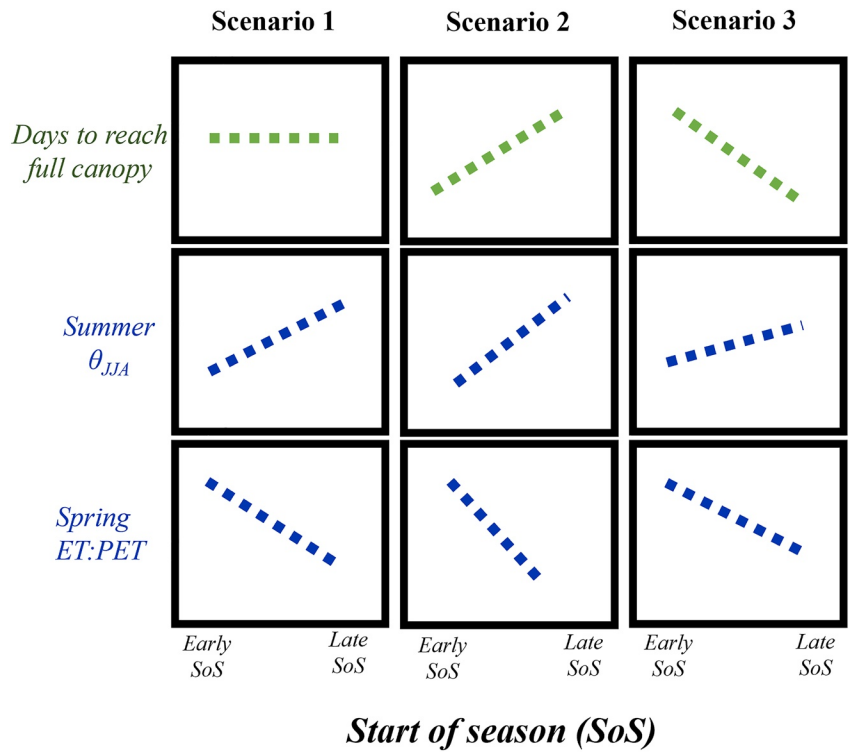

Figure 1. Three possible scenarios of canopy development and thus gross primary production and evapotranspiration (*ET*) trajectories. The pace of canopy development does not depend on start of spring (*SoS*) (scenario 1), canopy development is positively related to *SoS*, such that the canopy develops more rapidly when spring starts earlier (scenario 2), and canopy development is negatively related to *SoS*, such that canopy development progresses more rapidly when spring starts later (Scenario 3). These scenarios will influence the extent to which spring potential evapotranspiration (*PET*), *ET* and *ET:PET* will affect late summer soil moisture dynamics. In Scenario 1, early *SoS* could lead to low summer soil moisture and higher spring *ET:PET*, driven by the higher-than-average leaf area index (*LAI*). In Scenario 2, early *SoS* further exacerbates summer soil moisture stress due to even higher *LAI* and even greater spring *ET:PET*. In scenario 3, a more gradual pace of canopy development with earlier *SoS* weakens the impact of an early SoS on water cycling, by suppressing the springtime *ET:PET* compared with Scenarios 1 and 2.

pronounced for scenario 2, because the more rapid pace of canopy development results in a longer duration of high LAI, and thus more water extraction from the soil.

However, under scenario 3, an early start to spring would have smaller effects on water balance, because canopy development proceeds more slowly. When leaves emerge later (i.e., later *SoS*) under this scenario, *GPP* and *ET* reach their maximum potential more rapidly, which again weakens the relationship between *SoS* and soil water balance. These opposing responses could result in either exacerbated summer soil water deficits (as more water is removed from the soil in the spring) or will have no overall effect (as the cumulative amount of water moving from the soil to the atmosphere will roughly be equivalent). The potential for drought risk is increased with earlier *SoS* because as soil water depletion begins earlier, the ecosystem critically becomes more reliant on precipitation to maintain soil water resources for a longer duration. Given the predicted future increases in the frequency and severity of drought (Pendergrass et al., 2020), the need to better understand all factors contributing to drought intensification, including the dynamic role of vegetation phenology, is paramount. To the extent that a link between *SoS* and summer moisture deficits exists, our work could offer a new perspective on predicting moisture deficits several months in advance.

2. Materials and Methods

2.1. Site Descriptions

We used data collected from five flux tower sites in deciduous forests across the central and eastern United States: Coweeta Hydrologic Lab in Western North Carolina (US-Cwt, Oishi, Miniat, et al., 2018; Oishi, Novick,

Table 1
Site Details for Flux Tower Data Utilized

Site ID/data source	Elev. (m)	Climate	MAT (C)	MAP (mm)	Soil class	Years of data	Reference
US-Cwt AmeriFlux	670	Dfb	13	1,800	Clay loam	2011–2015	Oishi, Miniat, et al. (2018), Oishi, Novick, and Stoy (2018)
US-Dk2 AmeriFlux	168	Cfa	14.4	1,170	Silt loam	2002–2007	Novick et al. (2015)
US-MMS AmeriFlux	275	Cfa	10.9	1,030	Sandy clay	1999–2020	Roman et al. (2015)
US-MOz AmeriFlux	220	Cfa	12.1	985	Silt loam	2007–2017	Gu, Pallardy, Yang, et al. (2016)
US-Oho FLUXNET2015	230	Dfa	10.1	850	Sandy loam	2004–2013	Noormets et al. (2008)

et al., 2018), the Duke Forest hardwood site in central North Carolina (US-Dk2, Novick et al., 2015), the Morgan Monroe State Forest AmeriFlux site in southern Indiana (US-MMS, Roman et al., 2015), the Missouri Ozarks Ameriflux site (US-MOz, Gu, Pallardy, Yang, et al., 2016), and the Ohio Oak Openings site (US-Oho, Noormets et al., 2008) More details about these sites are presented in Table 1. These sites are generally not water-limited yet have experienced some degree of summer water stress according to the US Drought Monitor during their period of flux tower records (Novick et al., 2015; Stoy et al., 2008).

2.2. Eddy Covariance Measurement, Processing, and Quality Control

Eddy covariance (EC) systems were used to measure the net ecosystem exchange (NEE) of CO_2, latent heat flux (*LE*), sensible heat flux (*H*), wind speed (*u*), and friction velocity (*u**). Each EC system consisted of an infrared gas analyzer and a three-dimensional sonic anemometer, though instruments differ from site to site. At US-Cwt, an enclosed-path analyzer (EC-15; Campbell Scientific, Logan UT, USA) was paired with an RM Young 8100 sonic anemometer (RM Young Company, Traverse City, MI, USA). At US-Dk2, closed path gas analyzer (Licor-6262, Li-Cor, Lincoln NE, USA) was paired with a CSAT3 sonic anemometer (Campbell Scientific, Logan UT, USA). At US-MMS, a closed-path analyzer (LI-7000, LI-COR, Li-Cor, Lincoln NE, USA) was paired with a CSAT3 sonic anemometer (Campbell Scientific, Logan UT, USA). A side-by-side comparison of an LI-7500 and EC155 system revealed biases in the fluxes to be relatively low at US-Cwt provided that data collected with a high wind speed angle of attack were removed (Novick et al., 2013). At US-MOz, a fast response, open-path infrared gas analyzer (LI7500A; Li-Cor, Lincoln NE, USA) was paired with a RM Young 81000 sonic anemometer (RM Young Company, Traverse City, MI, USA). At US-Oho, an open-path infrared gas analyzer (LI-7500, Li-Cor, Lincoln NE, USA) was paired with a CSAT3 3-dimensional sonic anemometer (Campbell Scientific, Logan UT, USA).

Half-hourly or hourly fluxes were calculated from high-frequency data using site-specific algorithms. These are described for the US-Cwt in Oishi, Miniat, et al. (2018) and Oishi, Novick, et al. (2018), for the US-Dk2 site in Novick et al. (2015), for the US-MMS in Sulman et al. (2016), for the US-MOz site in Gu, Pallardy, Yang, et al. (2016), and for the US-Oho site in Noormets et al. (2008). These data were then submitted to AmeriFlux, where they were subjected to standardized quality control checks and then made accessible on the network websites (e.g., AmeriFlux or the global network FLUXNET). The flux tower records used in this study are quality-controlled records obtained from the networks (FLUXNET2015 or AmeriFlux) as described in Table 1. The data quality control and partitioning protocols for FLUXNET2015 are described in Pastorello et al., 2020. We used FLUXNET2015 GPP estimates produced by the nocturnal partitioning approach of Reichstein et al. (2005). The data obtained from AmeriFlux are not yet fully gapfilled or partitioned. Thus, for these datasets, gapfilled time series were generated from the Reddyproc software package (v.1.2.2; Wutzler et al., 2018). Data were filtered on the bases of friction velocity and gapfilled using a marginal distribution sampling approach. The measured carbon fluxes were also partitioned into *GPP* and ecosystem respiration within ReddyProc using the nocturnal partitioning approach of Reichstein et al. (2005). Finally, all measurements were aggregated to the hourly time scale for the comparative analysis.

2.3. Determining the Start of Spring (*SoS*) and Fraction of Total *GPP/ET*

We defined *SoS* as the first day in the season when the ratio of cumulative *GPP* (GPP_{Accum}) to the annual total (GPP_{ANN}), hereafter the GPP_{frac}, exceeded 25%. Mathematically, this variable can be expressed as:

$$GPP_{frac} = \frac{GPP_{Accum}}{GPP_{ANN}} \times 100\% \quad (1)$$

We repeated this analysis applying alternate thresholds to assess the sensitivity of *SoS* to these cutoffs, including when GPP_{frac} exceeded 10%, 15%, 20%, and 30%. The choice of the specific threshold did not strongly impact results (results not shown). The GPP_{Accum} represents a smoothed *GPP* record using a 14-day moving average. The ratio GPP_{frac} will be 0.25 when total *GPP* has reached 25% of the annual *GPP* (GPP_{25}), 0.50 when total *GPP* has reached 50% (GPP_{50}), 0.75 when total GPP has reached 75% (GPP_{75}), and 0.95 when total *GPP* has reached 95% (GPP_{95}), for a given year. This approach ensured that spurious excursions in *GPP* estimates in the early parts of the year (e.g., January or February) were not incorrectly interpreted as the *SoS*. We also computed a complimentary metric for ET (ET_{frac}).

$$ET_{\text{frac}} = \frac{ET_{\text{Accum}}}{ET_{\text{ANN}}} \times 100\% \tag{2}$$

where ET_{25}, ET_{50}, ET_{75}, and ET_{95} notations are analogous to those describing *GPP* fractions.

Seasonal means of θ, *ET*, *PET*, temperature, *P*, and vapor pressure deficit (*VPD*) were calculated and related to each other and the GPP_{frac} and ET_{frac}. Hereafter, "spring" refers to the period from day of year (*DOY*) 90–140, which encompasses the minimum and maximum *SoS* derived from *GPP,* while "growing season" refers to the period between *DoY* 180–250.

2.4. Estimated Potential *ET* (*PET*)

We used the Penman-Monteith equation (Allen et al., 1994) to estimate potential evapotranspiration (*PET*):

$$PET = \frac{\Delta \times R_n \times \complement_\rho \times \rho_a \times g_a \times VPD}{L_v \times 1000 \times \rho_w \times \left(\Delta + \gamma \times \left(\frac{1+g_a}{gc_{\text{ref,ww}}}\right)\right)} \tag{3}$$

where Δ is the slope of saturation water vapor function (kPa K^{-1}), R_n is net radiation (W m^{-2}), $\complement_\rho$ is the specific heat capacity of dry air (J kg^{-1} K^{-1}), ρ_a is the density of dry air (kg m^{-3}) g_a, is the aerodynamic conductance (m s^{-1}), *VPD* is the vapor pressure deficit (kPa) of the atmosphere, L_v is the latent heat of vapourization (kJ K^{-1}), ρ_w is the density of water (kg m^{-3}), γ is the psychrometric constant (kPa K^{-1}), and $gc_{\text{ref,ww}}$ is a reference canopy conductance (m s^{-1}) for well-watered, high light conditions when soil moisture is close to saturation. Surface conductance can be obtained by inverting measured *ET* fluxes using the Penman-Monteith equation (Whitley et al., 2009). The $gc_{\text{ref,ww}}$ was then calculated as the average surface conductance when *VPD* was between 0.8 and 1.2 kPa, R_n was >500 W m^{-2}, and $GPP > 0.75$ of maximum value.

To evaluate the vegetative contribution to overall spring *ET*, we calculated the ratio of springtime *ET* to springtime *PET.*

$$ET{:}PET = \frac{ET}{PET} \tag{4}$$

To the extent that *ET* is controlled by *LAI*, then the spring *ET:PET* for a given DOY will be larger when *LAI* is relatively high. We also explored links between *SoS* and the ratios of *ET* to precipitation (*ET:P*), and *PET* to precipitation (*PET:P*). Jointly analyzing the dynamics of *ET:P* and *PET:P* also permits a disentanglement of the role of canopy development from interannual variability in spring climate; specifically, canopy development should more directly impact *ET:P* than *PET:P*. Importantly, however, both of these ratios also account for the contribution of water inputs (e.g., *P*) to the overall site water balance.

θ was measured using water content reflectometry probes within the top 0–30 cm of soil (CS615 and CS616; Campbell Scientific Inc.). To standardize soil water content to reflect the range typically experienced by an individual site, we converted volumetric water content into relative extractable water using the equation

$$\theta_{\text{rel}} = \frac{\theta_{\text{measured}} - \theta_{\text{min}}}{\theta_{\text{max}} - \theta_{\text{min}}} \tag{5}$$

where θ_{measured} is the half-hourly average of volumetric soil water content (*VWC*), θ_{min} is the annual minimum of *VWC*, and θ_{max} is the annual maximum measured of *VWC*.

Throughout the text, the $\theta_{[\text{rel,month}]}$ notation is retained when referring to mean soil moisture of different months.

2.5. Ground-Based and Species-Level Phenology Metrics

We relied on two ground-based phenological datasets to provide an independent check on the results emerging from the tower derived data. The first was a 21-year- record of ground-based *LAI* measurements taken every 1–2 weeks in the footprint of the US-MMS flux tower along three transects (NW, SW, W) with a LAI-2200 (LiCOR, Lincoln, NE, USA). Measurements begin early in the year, well before any budbreak occurs, and continue until winter, as described in Roman et al. (2015).

The *LAI* data were used to determine an independent estimate of canopy-scale *SoS*. Specifically, in an approach analogous to determining start of sprint from the GPP records, we fitted a sigmoidal function to the annual *LAI* record from each of the 21 years, and then defined *SoS* as the *DoY* when *LAI* reached a value equal to 25% of the difference between annual minimum and maximum *LAI* (hereafter $SOS_{LAI,25}$). Next, we repeated this exercise using *LAI* measurements taken through May (*DoY* 120), but then replacing *LAI* observations collected after *DoY* 120 with the 21-year mean *LAI* for June, July, and August (hereafter $SOS_{LAI,\mathrm{mean}}$). This second estimate is motivated by our study's focus on understanding the extent to which phenology dynamics in early spring might predict the likelihood of growing season moisture deficits. For the *SoS* to be used in a predictive sense, it is useful to define *SoS* in a way that does not rely on summer month (e.g., June, July, August) *LAI* measurements. Both of these *LAI*-derived *SoS* metrics were then compared to the estimates of *SoS* derived from *GPP*. We quantified the residuals of the relationship between *SoS* determined from modeled *LAI* and each derived *SoS* from GPP_{20}, GPP_{25}, and GPP_{30} from the 1:1 line to ensure use of the *GPP* metric with the least residuals. We used linear regression analysis to determine the relationship of each modeled *LAI SoS* to each *GPP* metric. Finally, the *LAI* data were also used to evaluate the relationship between $SOS_{LAI,25}$ and the pace of canopy development, in this case defined as the number of days between the $SOS_{LAI,25}$ and the *DoY* each year at which peak *LAI* was reached.

The second data set includes species-specific observations of phenophase using protocols based on those developed by the National Ecological Observatory Network (NEON) and described in Jones (2022). Specifically, in early spring of 2021, we established a 100 × 100 m square "loop" transect in the US-MMS tower footprint and tagged 120 trees within 1–5 m from the transect for routine phenophase monitoring. This set of 120 trees contained 12 unique species, including *Acer saccharum* (sugar maple, $N = 36$), *Liriodendron tulipifera* (tulip poplar, $N = 30$), *Ulmus americana* (American elm, $N = 17$), *Sassafras albidum* (sassafras, 11), *Fagus grandifolia* (American beech, $N = 7$), *Quercus alba* (white oak, $N = 5$), and fewer than four individuals of *Prunus serotina* (black cherry), *Robinia pseudoacacia* (black locust), *Nyssa sylvatica* (black gum), *Celtis occidentalis* (hackberry), *Quercus rubra* (red oak), and *Quercus muehlenbergii* (chinkapin oak). From March to April of 2021, we recorded the phenophase at each site twice weekly, with measurements were made 3 times a week from April to June. Phenophase categories included: (a) breaking leaf buds (e.g., a green leaf tip is visible at the end of the bud), (b) increasing leaf size (e.g., leaves have not yet reached their full size), (c) leaf presence (e.g., the presence of live, unfolded leaves), and additional categories describing flowering status and the extent of autumn leaf color change. In all cases, the intensity of each phenophase was monitored using a percentile scale (<5%, 5%–24%, 25%–49%, 50%–74%, 75%–94%, ≥95%).

We analyzed tree-level observations from the first two categories (budburst and increasing leaf size), primarily to evaluate species-specific relationships between the start of the growing season and the pace of canopy development. The tree-level *SoS* was estimated as the day when visible "breaking leaf buds" phenophase were first recorded (usually, as <5% or 5%–24%). The tree-level data were also analyzed to determine the *DoY* when each tree canopy was intermediately developed (defined as the *DoY* when the "increasing leaf size" phenophase was first recorded to be 25%−49%), and when each tree canopy was fully developed (defined as the *DoY* when the "increasing leaf size" phenophase was first recorded to be ≥75%−94%). The pace of canopy development was then related to the number of days between the tree-level *SoS* and the *DoY* of "intermediate" or "full" canopy development. The tree-level *DoY* associated with budburst, intermediate and full canopy development were randomly jittered to within a 3-day period preceding the actual measurement date. This step improves data visualization, but also reflects the fact that phenophase development could have happened earlier than it was observed with our twice-weekly sampling strategy.

2.6. Statistical Analysis

Statistical analyses were performed using MATLAB (R2020a, The MathWorks, Inc, Natick, Massachusetts, USA) and we considered an alpha-level of 0.05 ($\alpha = 0.05$) to be statistically significant for all analyses. We used

multiple linear regression analysis to determine the effects of site, *SoS*, and spring temperature (Ta_{spr}) on summer (June–August) soil moisture ($\theta_{rel,JJA}$), with site as a categorical variable. The full model took the form as:

$$\theta_{JJA} \approx 1 + \text{site} + SoS + Ta_{spr} + PET + ET\,\text{ratio} + ET_{50} + ET_{95} + \text{interactions} \quad (6)$$

The interactions term in Equation 6 incorporates all possible interactions of each of the included variables. Variables were considered not important at an alpha level <0.05 and were subsequently removed (See SI1 in Supporting Information S1 for stepwise removal of NS variables/interactions) to simplify the model which took the form of:

$$\theta_{JJA} \approx 1 + SoS + Ta_{spr} + PET + SoS \times Ta_{spr} + SoS \times PET + PET \times Ta_{spr} \quad (7)$$

We applied the model using a seasonal average of $\theta_{\mathbf{rel,JJA}}$(mean June, July, and August). Additionally, we performed the linear regression using the individual mean monthly values of soil moisture (e.g., $\theta_{rel,APR,}$ $\theta_{rel,MAY}$, $\theta_{rel,JUN}$, $\theta_{rel,JUL}$, and $\theta_{rel,AUG}$) in addition to the seasonal averages. Because summer soil moisture dynamics will directly reflect the balance of water inputs and removals from the ecosystem, we also applied an analogous regression model to evaluate how *SoS* affected the ratio of annual *ET* to annual precipitation (*P*) as well as monthly *ET:P* ratios (April, May, June, July, August, and JJA). We also explored the impact that *SoS* had on the rate at which *GPP* and *ET* increased throughout the season by determining the *DoY* that incremental percentages of each (*GPP*, *ET*) were achieved (50%, 75%, and 95% to cumulative total *GPP* and *ET*).

3. Results

3.1. Relationship Between *SoS* and the Acceleration of *ET* and *GPP* in Spring

Ecosystem *GPP* increases more rapidly when the *SoS* occurs later (Figures 2a–2c; $p < 0.01$). Specifically, the time required for GPP_{frac} to reach 50%, 75%, and 95% was linearly and negatively related to the *SoS*. Moreover, the slope of those relationships becomes steeper (i.e., more negative) as the dependent variable progresses from GPP_{frac} of 50% (GPP_{50}) to GPP_{frac} of 95% (GPP_{95}, $m = -0.56$ days/days and $m = -1.2$ days/days), respectively.

Likewise, years with later *SoS* exhibit more rapid acceleration to achieve ET_{50}, ET_{75}, and ET_{95} (Figures 2d–2f; $p < 0.001$). Again, the slope of those relationships becomes more negative as the dependent variable progresses from ET_{frac} of 50% to ET_{frac} of 95% ($m = -0.63$ days/day and $m = -0.82$ days/days), respectively (Figures 2d and 2f).

3.2. The Relationship Between Spring Canopy Development and Summer Soil Water

Across all sites, *SoS* was a significant predictor of spring *ET:PET* (Figure 3b; $F_{49,51} = 16.5$; $R^2 = 0.17$ $p < 0.01$), explaining 20% of the variability, with spring *ET:PET* declining linearly as the *SoS* occurred later. At US-MOz, *SoS* was a significant predictor of spring *ET:PET* (Figure 3a), explaining 44% of its variability. However, the only site where *SoS* was a significant predictor of both spring *ET:PET* (Figure 3a) and $\theta_{rel,JJA}$ (Figure 3c) was US-MMS, which was the site with the most data available (22 years). In US-MMS, *SoS* explained 35% of the variability in *ET:PET* (Figure 3a; $F_{19,21} = 9.71$; $R^2 = 0.35$; $p < 0.05$) and 22% of the variability in mean summer $\theta_{rel,JJA}$ (Figure 3c.; $F_{19,21} = 5.41$; $R^2 = 0.22$; $p < 0.05$). Across all sites, *SoS* was not a significant predictor of summer soil moisture, regardless of whether the summer soil water data was evaluated as θ_{rel} (Figure 3d; $p = 0.65$) or the raw measured volumetric moisture content ($p = 0.31$, *data not shown*).

Through a multilinear regression, we aimed to find the most parsimonious model for summer soil moisture using spring observations, to serve as an early indication of summer plant water stress. Using site as a categorical variable for *SoS, spring PET,* Ta_{spr}, and their interactions as predictor variables, we determined that retaining these variables yields a significant model which explains ~52% of the variability in $\theta_{rel,JJA}$ (Table 2). *SoS*, spring *PET*, and their interactions each emerged as being significant predictors of $\theta_{rel,JJA}$ ($p < 0.05$). Ta_{spr} only emerged as significant in the interaction with spring *PET* ($p = 0.044$) but not significant as a single predictor, nor with respect to its interaction with *SoS* ($p > 0.1$).

In US-MMS, the *SoS* has no effect on $\theta_{rel,APR}$ or $\theta_{rel,MAY}$ (Figures 4a and 4b; $p = 0.24$ and 0.50, respectively), but explains ~18–20% of the variability in $\theta_{rel,JUN}$, $\theta_{rel,JUL}$, $\theta_{rel,AUG,}$ and $\theta_{rel,JJA}$ (Figures 4c–4e; $p = 0.07$, 0.05, 0.09, and 0.04, respectively), and ~22% of variability for the months of June - August collectively.

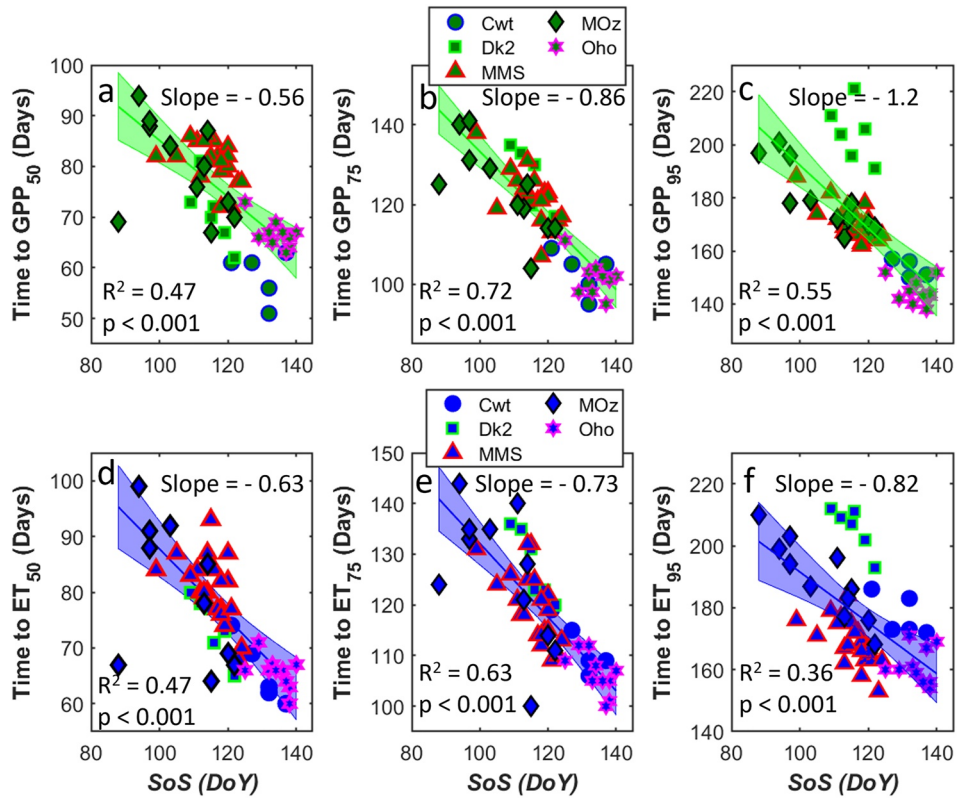

Figure 2. The number of days since start of spring for GPP_{frac} to equal (a) 50%, (b) 75%, and (c) 95%, and the time it takes for ET_{frac} to equal (d) 50%, (e) 75%, and (f) 95%. Each panel demonstrates that as spring leaves emerge later in the season, the time it takes to achieve these incremental percentages of carbon uptake and evapotranspiration occurs more quickly (i.e., the plants are catching up).

3.3. The Relationship Between Spring Canopy Development and Spring *ET* Dynamics

In US-MMS, *SoS* explained 35% of the variability in the annual ratio of *ET* to precipitation (*ET:P*; Figure 5f; $p < 0.005$). We explored how this ratio varied across selected months with *SoS* explaining 40%, 27%, 40%, 40%, and 40% of the variation in the ratio of *ET:P* for the months of April - August, respectively (Figures 5a–5e; $p < 0.004$). Similarly, *SoS* explained ~41% of the annual variation in the ratio of *PET* to precipitation (*PET:P*; Figure 6f; $p = 0.001$), and 21%, 27% 30%, 36%, and 37% of the variation for the months April - August (Figures 6a–6e; $p < 0.08$). The changing trends in *ET:P* and *PET:P* with *SoS* were mostly generalizable in other sites as well (Table 3). Negative slopes emerged in *ET:P* for *DoY* 90–130 and June–August in US-Cwt, for *DoY* 90–130 in US-Dk2, for each time period excluding July in US-MOz, and each time period in US-Oho. Negative slopes emerged in *PET:P* for April–August in US-Cwt, for *DoY* 90–130 in US-Dk2, for each time period excluding April and May in US-MOz, and July - August in US-Oho. These results did not, however, translate into a higher spring *ET:PET* ratio or lower $\theta_{rel,JJA}$ with early *SoS* ubiquitously. In both US-Oho and US-MOz, negative slopes emerged in *DoY* 90–130 for *ET:PET*, and for April and May in US-MOz; although surprisingly, this did not result in a positive slope for $\theta_{rel,JJA}$ as a function of *SoS*. In other words, a higher spring *ET:PET* ratio in US-MOz and US-Oho did not result in lower mean soil moisture in the summer.

3.4. Relationship Between Tower-Derived and Ground-Based Phenology Records

The *GPP*-derived *SoS* (e.g., $SoS_{GPP,25}$) generally agrees well with the *SoS* estimated from the ground-based *LAI* data (e.g., $SoS_{LAI,25}$, Figure 7a, $R^2 = 0.48$, $p < 0.001$, slope = 0.40). When the measured summertime (June, July, August) *LAI* in each year is replaced with the mean value across the 21-year-long-record, the relationship still clear (Figure 7b, $R^2 = 0.67$, $p < 0.001$, slope = 0.77). This result suggests that observations of leaf area made in spring can still be used to estimate the *SoS* even before the onset of the growing season, provided some information about mean summertime *LAI* is available (e.g., from remote sensing or historic observations).

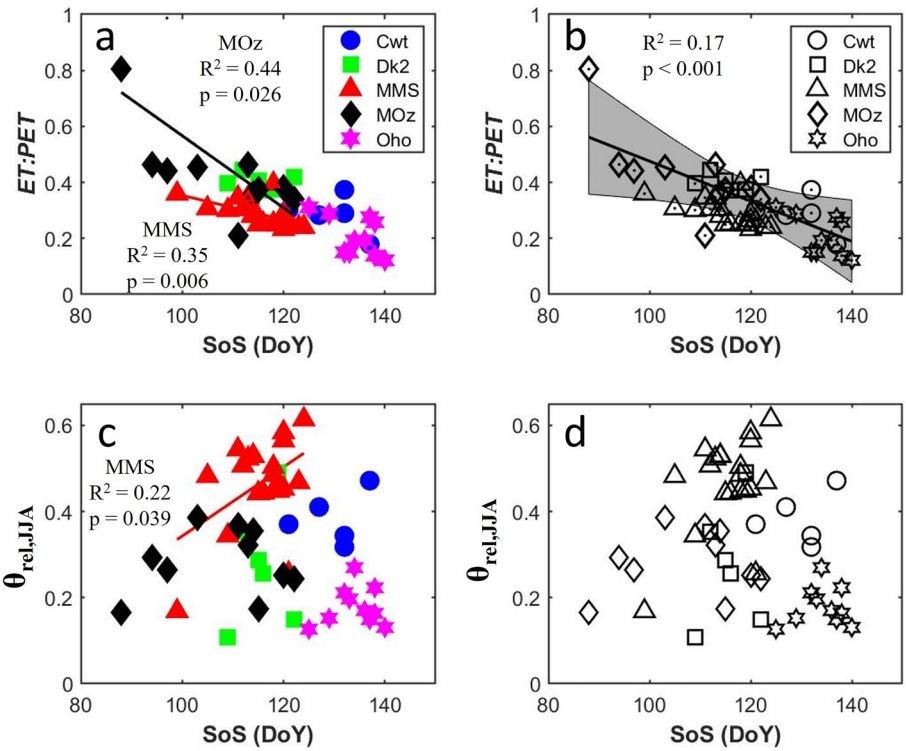

Figure 3. The spring evapotranspiration: potential evapotranspiration (*ET:PET*) (a) and mean summer (June–August) θ (c) as a function of the start of spring *(SoS)*, demonstrating *SoS* as a good indicator of each response variable at MMS ((a), (c); red triangles) and for spring *ET:PET* across all sites when data are pooled (b). The relationship disappears when pooling θ_{JJA} across sites (d) suggesting that effects on θ_{JJA} results are not generalizable.

Finally, the ground-based phenology data confirm the negative relationship between *SoS* and the pace of canopy development (Figure 8). This relationship emerges from both the species-specific phenophase observations (Figures 8a and 8c) and the canopy-scale *LAI* data record (Figures 8b and 8d).

4. Discussion

4.1. The Compensatory Nature of Ecosystem Scale Processes

We aimed to determine the degree to which ecosystem carbon and water cycling were affected by phenological shifts in spring vegetation. Our results demonstrate that more rapid canopy development when spring comes later causes cumulative *GPP* and *ET* to accelerate quickly, which compensates for reductions in these fluxes linked to later leaf emergence. As a consequence, *GPP* and *ET* reach their maxima on approximately the same DOY, regardless of when leaf emergence occurs (Figure 2). Specifically, the later in the season that spring begins, the time it takes *GPP* and *ET* to reach their full potential (e.g., GPP_{95} and ET_{95}) decreases, supporting scenario 3 (Figure 1). In other words, the ecosystem effectively "catches up" from the delayed start to the season, which minimizes the impact of *SoS* on annual *GPP* and *NEE* for eastern temperate forests. More gradual canopy development with earlier *SoS* (and more rapid development with later *SoS*) reduces the sensitivity of annual *GPP* to spring phenological timing, as the leaves that emerge early make small contributions to overall *GPP*. This would indicate that *SoS* alone will not directly explain increases (when early) or decreases (when late) in *GPP* but would instead have a more indirect effect dependent on the interplay between consistent optimal temperatures for growth and timing of growth onset. However, even when favorable conditions (i.e., temperature)

Table 2
Multiple Linear Regression Results for Predicting Mean Summer θ

	Estimate	SE	t-stat	p-value
Intercept	4.743	1.718	2.761	0.008
SoS	−0.039	0.014	−2.809	0.007
sprTa	−0.111	0.106	−1.041	0.304
PET	−0.008	0.002	−4.527	<0.001
SoS:sprTa	0.001	0.001	1.431	0.160
SoS:PET	<0.001	<0.001	4.911	<0.001
sprTa:PET	−0.000	<0.001	−2.072	0.044

Note. Number of observations: 51, Error degrees of freedom: 44; Root Mean Squared Error: 0.107; R-squared: 0.521, Adjusted R-Squared: 0.456; F-statistic versus constant model: 7.99, p-value = 7.4e−06.

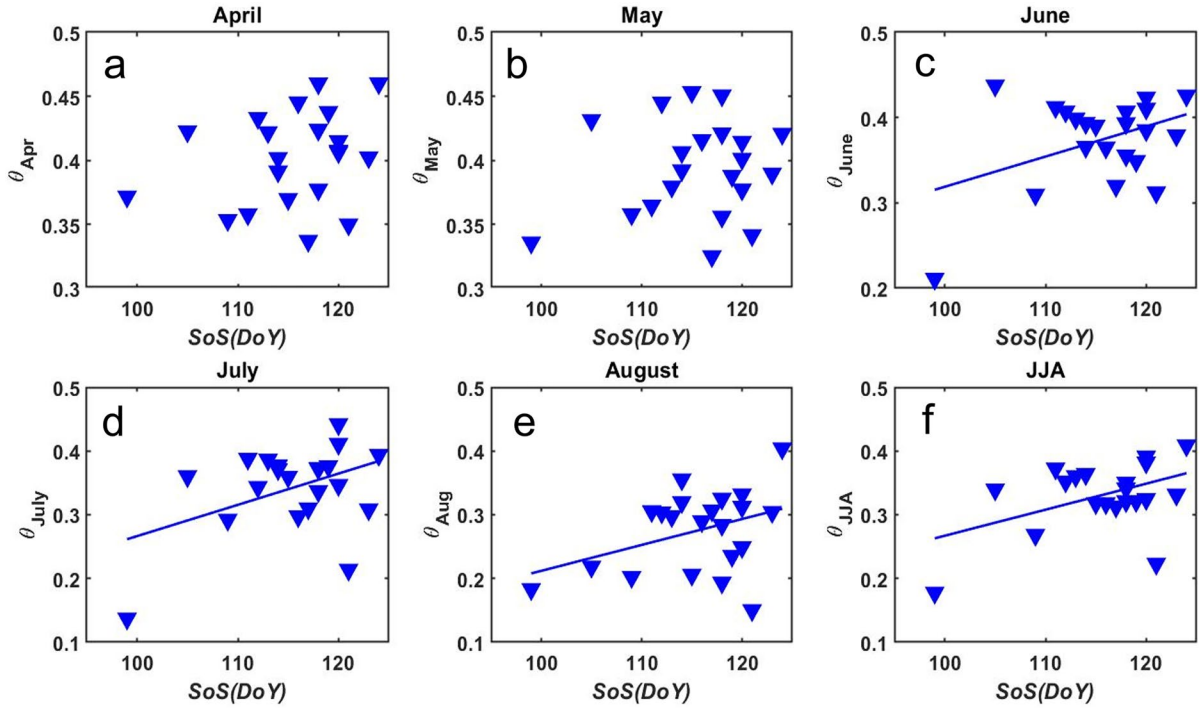

Figure 4. Summer monthly mean soil moisture as a function of start of spring (*SoS*) at US-MMS. *SoS* does not appear to have any influence over $\theta_{rel,APR}$ or $\theta_{rel,MAY}$ (panels (a) and (b)); however, as the summer progresses into June and July (panels (c) and (d)), SoS emerges as a moderately good indicator of $\theta_{rel,}$ and becomes increasingly important moving into August (panel (e)) when *SoS* explains ~22% of the variation (see Table 3 for regression results. Parameter estimates are presented in SI2 in Supporting Information S1).

and growth onset coincide in the spring, which would be advantageous for maximizing annual growth and possibly resulting in rapid canopy development, the link will likely be weakened with soil moisture deficits limiting growth in the fall (Buermann et al., 2018). This result is consistent with prior work at the tree-level, which showed that for several deciduous tree species growing in the northern hemisphere, earlier budbreak was

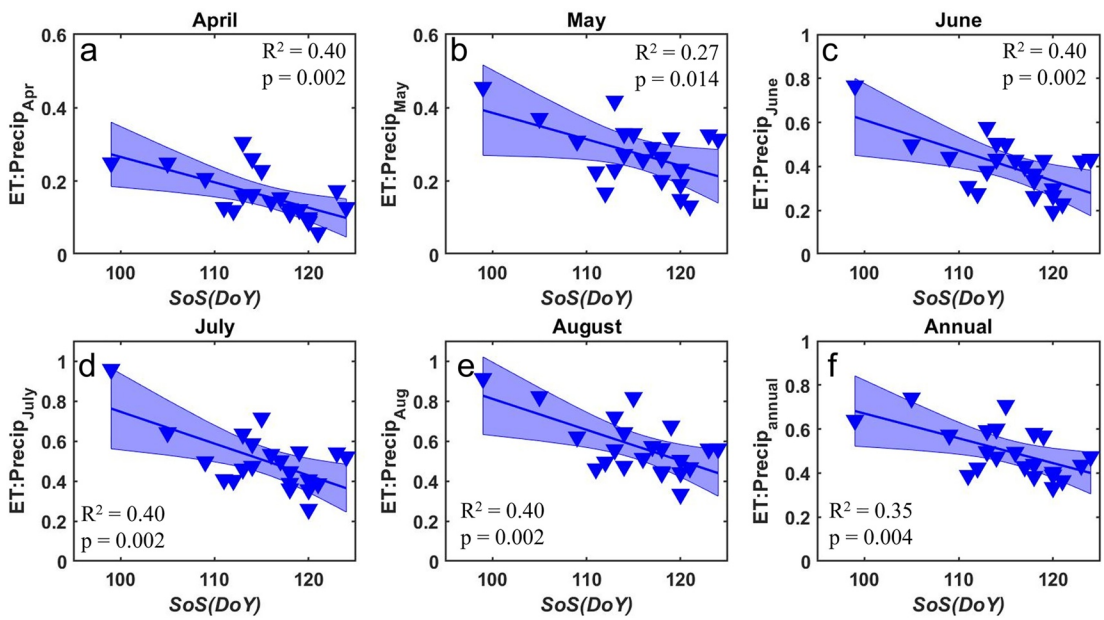

Figure 5. The ratio of evapotranspiration (*ET*) to precipitation as a function of start of spring (*SoS*) at US-MMS indicating that a greater proportion of water that falls as precipitation is returned to the atmosphere via *ET* during each of the months April–August (a–e) as well as annually (f) in years that the *SoS* occurs earlier.

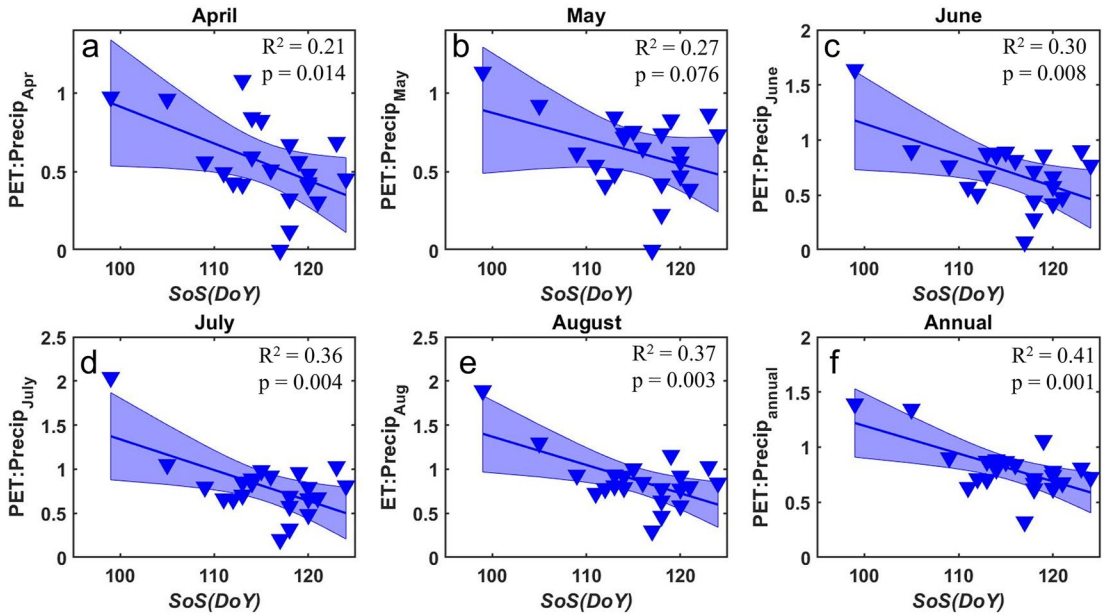

Figure 6. The ratio of potential evapotranspiration to precipitation as a function of start of spring (*SoS*) at US-MMS MMS indicating that a greater proportion of water that falls as precipitation has the potential for being returned to the atmosphere via evapotranspiration during each of the months April–August (a–e) as well as annually (f) in years that the *SoS* occurs earlier.

related to a longer green-up period (Klosterman et al., 2018). Importantly, this relationship was independently confirmed using tree-level phenophase data (Figures 8a and 8c) and ground-level *LAI* observations (Figures 8b and 8d). In springs when the start of the season occurs much earlier than normal, it is more likely that temperatures will fluctuate, varying from optimal to sub-optimal conditions for growth as well as an increased potential for vegetation-damaging late frost events, which is detrimental to plants with foliage (Gu et al., 2008; Vitasse et al., 2014). A slower rate in the development of canopy is more likely under these conditions, which could delay advancement to maximum *ET*. These results, observed for sites that generally have abundant soil moisture throughout the spring months, may not necessarily hold in more arid biomes, where leaf area and soil moisture are more tightly coupled (Byrne et al., 2020).

Modeling studies suggest that while we will continue to expect earlier *SoS* as springs become warmer, individual species' sensitivity of leaf-out to temperature is highly variable (Morin et al., 2009; Polgar & Primack, 2011; Vitasse et al., 2009). Thus, species composition will affect the degree to which ecosystem-scale processes develop, particularly when considering risk of late spring frost (Hufkens et al., 2012); and although Zohner et al. (2020) report that late spring frost *risk* has decreased in North America over the last 50 years, frost *damage* has increased over the past ∼120 years (Augspurger, 2013). In temperate forest ecosystems, earlier *SoS* due to warming does not always translate into a longer growing season length (Dragoni et al., 2011) but simply a shift in timing (Richardson et al., 2010). Indeed, Dow et al. (2022) demonstrate that spring temperatures had no consistent effect on annual growth, peak growing season length, or maximum growth rates, although the timing of stem diameter growth occurred earlier.

4.2. The Interacting Role of Phenology and Meteorology for Summer Soil Water Deficits

We focus the discussion of the interacting role of phenology and meteorology on US-MMS, which is the site with the longest data record. In this site, the *ET:P* and *PET:P* decreased with increasing *SoS* (Figures 5a–5e). Exploring the difference between *ET:P* and *PET:P* can help to disentangle the direct influence of phenological timing, which should primarily affect *ET*, from year-to-year variability in meteorological drivers that may enhance both spring *PET* and *ET*. In US-MMS, the relationship between *SoS* and *ET:P* is stronger than the relationship between *PET:P* for April, May, and June, but not for July and August (compare Figures 5 and 6). This result is consistent with the expectation that phenology-driven increases to *LAI* play an important role in governing the dynamics

Table 3

Slope Parameter Results From Linear Regression Models Between SoS and Mean θ_{rel}, ET:PET, ET:P, and PET:P for DoY 90–130, Monthly (April–August), JJA, and Annually

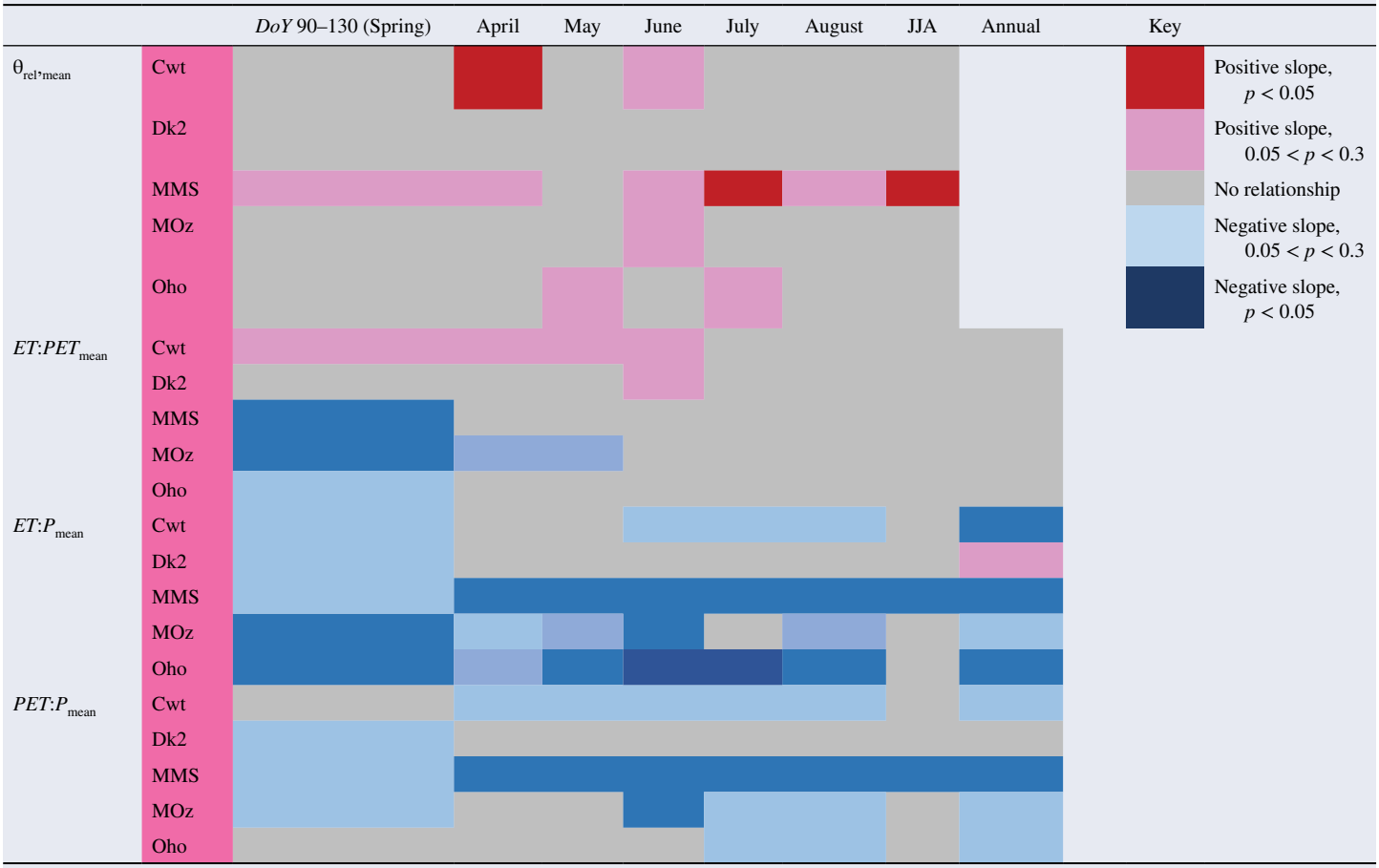

Note. See key for colors indicators of significance levels of each result. SoS, Start of Spring; ET, evapotranspiration; PET, potential evapotranspiration.

of *ET* during months when *LAI* is typically dynamic (e.g., the shoulder seasons, April–June) as opposed to months during which *LAI* is usually quasi-static (e.g., July, August). In contrast, annual growth (e.g., ring-width) tends to be sensitive to climate conditions (e.g., temperature and precipitation) within the growing season (Dow et al., 2022). However, it is clear that climate-driven variability in *PET* alone is substantial and could increase spring *ET* even in the absence of dynamic phenological timing. Thus, at least in this site, the consequence for summer soil moisture reflects both interannual climate variability and variability in the timing and pace of canopy development.

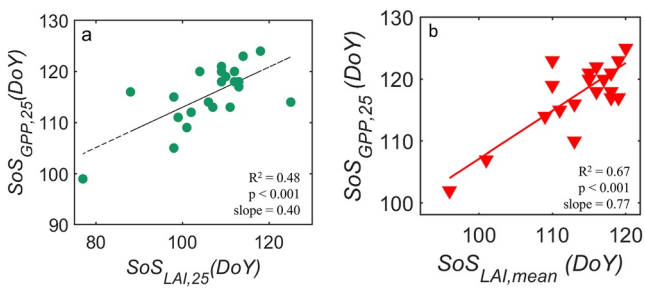

Figure 7. Panel (a) shows the relationship between the start of spring (*SoS*) estimated from the gross primary production records ($SOS_{GPP,25}$) versus the *SoS* estimated from the ground-based leaf area index (*LAI*) records ($SOS_{LAI,25}$) defined as the *DoY* when *LAI* crosses 25% of maximum. Panel (b) shows the same relationship but using long-term averaged *LAI* ($SoS_{LAI,mean}$) data for June–July–August to better understand the extent to which *SoS* can be predicted using springtime measurements alone.

Moreover, if summer precipitation is also limited during years with an early *SoS*, this could create a scenario leading to exacerbated summer soil water deficits. At US-MMS in 2012, conditions were such that *SoS* was 9 days sooner than the next earliest *SoS* (18 days sooner than the 22-year mean); moreover, during June and July, the site received only 23 mm of rainfall, which is less than 10% of the long-term mean (Yi et al., 2017). This is a critical consideration given that these climate conditions will likely occur more frequently in the future, with projections of warmer and drier summers.

While results from US-MMS are compelling, these patterns were not generalizable across sites, which can at least partly be explained by shorter tower records at those sites, which should motivate sustained investment in

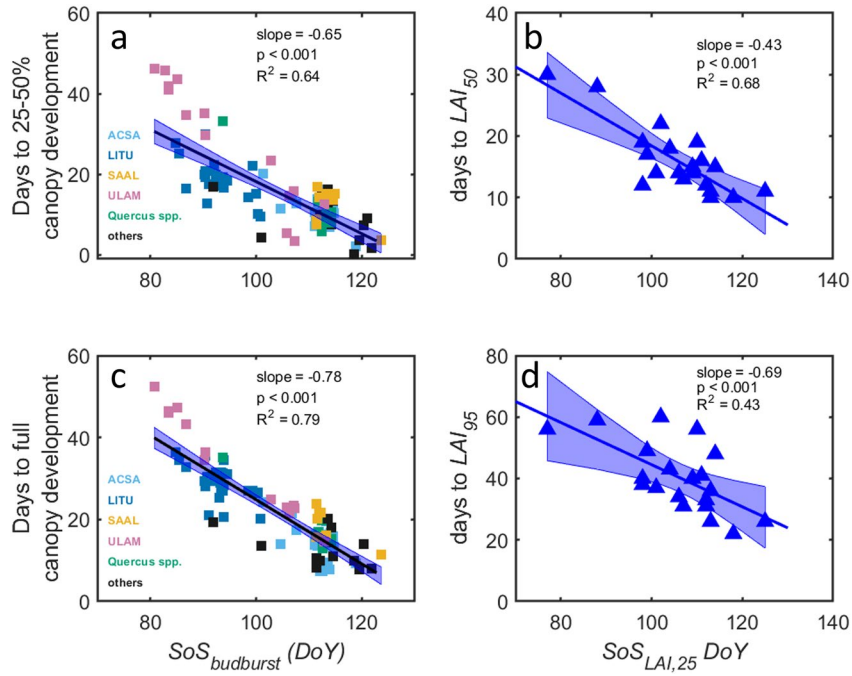

Figure 8. Panel (a) shows the tree-level relationships between the number of days until each tree canopy was intermediately developed, and the start of spring estimated as the *DoY* of budburst. Panel (b) shows the relationship between number of days for ecosystem-scale leaf area index (*LAI*) to reach 50% (LAI_{50}) of its peak value in a given year, and the *DoY* when the *LAI* exceed 25% of this peak ($SoS_{LAI,25}$). Panel (c) shows the same relationship as panel (a) but for full tree-level canopy development. Panel (d) shows the same relationship as panel (b), but for full *LAI* development. In panels (a) and (c), species codes are as follows: ACSA, *Acer saccharum*; *LITU*, *Liriodendron tulipifera*; *SAAL*, *Sassafras albidum*; ULAM, *Ulus americana*; QUERCUS spp, (*Quercus alba*; *Quercus rubra, Quercus velutina*, *and Quercus muehlenbergii*); and OTHER, all other species.

generating long-term flux tower time series. The 20+ year record at US-MMS showed a wide range of *SoS* from the earliest *DoY* 99 to the latest *DoY* 124, resulting in a 25-day difference over the 22-year record. With the exception of US-MOz, which had a 34-day difference in earliest to latest *SoS* (over a 10-year record), other sites had a shorter range in *SoS* with a 16, 13, and 15-day range for US-Cwt, US-Dk2 and US-Oho, respectively. It is worth considering not only the amount of rainfall but the variability in precipitation events (e.g., intensity and timing), as this will affect how much water is ultimately available for plant use (Gu, Pallardy, Hosman, et al., 2016) and will also impact tree growth (Elliott et al., 2015).

4.3. SoS as Potential Early Indication of Summer Soil Water Deficits

We explored the potential to use *SoS* in any given year as an indicator for summer soil moisture deficits and likelihood of plant water stress in the late growing season. To support the goal of using *SoS* as a predictor of soil moisture deficits, we present an approach to estimate *SoS* informed solely by *LAI* measurements, which does not require annual records of C fluxes. If *SoS* emerges as a relevant predictor, then this information could be used as an early drought warning signal. In US-MMS, ~20% of the variation in mean summer θ could be explained using only *SoS*. This increased to ~32% when we added site as a categorical variable and spring *PET* and Ta_{spr} as explanatory variables. It is important to note that, to some extent, *SoS* reflects the biological response to springtime meteorological conditions (as reflected by *PET* and Ta_{spr}), and thus it is not surprising to see that the interaction between *SoS* and *PET* emerged as a significant driver in the model (though the interaction between *SoS* and Ta_{spr} did not). Thus, the most robust predictive model for summer soil moisture should consider information on both phenological timing and also springtime *PET*.

These are variables readily observable, in near-real time, from remote sensing and weather station networks, which would support future work to explore the extent to which these patterns are generalizable at regional scales (an analysis that would benefit from timeseries that are longer than those provided by most flux towers

to date). Since our *SoS* was calculated from aboveground observations, it is important to note that above- and below-ground phenology do not track equivalently (Abramoff & Finzi, 2015). In fact, root growth lags behind shoot growth in woody plants (Steinaker et al., 2010) and the soil depth that roots are able to reach (thus access to deeper held soil water) is an important factor in whether plants experience hydrologic stress, which is not always reflected by the moisture measured in the top 30 cm of the soil. However, the ability to incorporate easily observable springtime conditions (i.e., *SoS*, temperature, etc.) into an indication of expected conditions of plant available water throughout the summer can help land managers to be better prepared for the potential of insufficient water resources.

5. Conclusions

While early springtime transpiration linked to early leaf emergence can increase the risk of summer drought, adjustments in the rate of canopy development can compensate for increases in transpiration, alleviating some of the pressure on growing season water supply. However, this compensation may not be sustained if future climate conditions are characterized by increases in spring temperatures and *PET*, which will further enhance springtime *ET* and thus further deplete summer soil moisture in regions like the Eastern US, where soils saturate over winter and then gradually dry over the course of the growing season.

Data Availability Statement

AmeriFlux data used in this analysis are available at https://ameriflux.lbl.gov/, and the data set citations for each site are provided in Table 1. FLUXNET2015 data used in this analysis are available at FLUXNET2015 Data set - FLUXNET (https://fluxnet.org/data/fluxnet2015-dataset/). Data analysis was performed in MATLAB (R2020a, The MathWorks, Inc, Natick, Massachusetts, USA). The code for performing analysis is available.

Acknowledgments
The findings and conclusions in this publication are those of the authors and should not be construed to represent any official USDA or U.S. Government determination or policy. Funding for the work was provided by USDA NIFA (award # 2021-67034-35129) and the NASA FINESST Program (award 20-EARTH20-143). AmeriFlux data were made available through the data portal (https://ameriflux.lbl.gov) and processing maintained by the AmeriFlux Management Project, supported by the U.S. Department of Energy Office of Science. We acknowledge Mike Voyles, Steve Scott, Tracy Mai, Daniela Cala, Daniel Beverly, and Michael Benson for their help collecting the ground-based phenological data at Morgan-Monroe, and Tyler Roman and Mike Voyles for their continuous collection of LAI data.

References

Abramoff, R. Z., & Finzi, A. C. (2015). Are above-and below-ground phenology in sync? *New Phytologist*, *205*(3), 1054–1061. https://doi.org/10.1111/nph.13111

Allen, R. G., Smith, M., Pereira, L. S., & Perrier, A. (1994). An update for the calculation of reference evapotranspiration. *ICID Bulletin*, *43*(2), 35–92.

Augspurger, C. K. (2013). Reconstructing patterns of temperature, phenology, and frost damage over 124 years: Spring damage risk is increasing. *Ecology*, *94*(1), 41–50. https://doi.org/10.1890/12-0200.1

Blanken, P. D., & Black, T. A. (2004). The canopy conductance of a boreal aspen forest, Prince Albert National Park, Canada. *Hydrological Processes*, *18*(9), 1561–1578. https://doi.org/10.1002/hyp.1406

Buermann, W., Forkel, M., O'sullivan, M., Sitch, S., Friedlingstein, P., Haverd, V., et al. (2018). Widespread seasonal compensation effects of spring warming on northern plant productivity. *Nature*, *562*(7725), 110–114. https://doi.org/10.1038/s41586-018-0555-7

Byrne, B., Liu, J., Bloom, A. A., Bowman, K. W., Butterfield, Z., Joiner, J., et al. (2020). Contrasting regional carbon cycle responses to seasonal climate anomalies across the east-west divide of temperate North America. *Global Biogeochemical Cycles*, *34*(11), e2020GB006598. https://doi.org/10.1029/2020gb006598

Cleland, E. E., Chuine, I., Menzel, A., Mooney, H. A., & Schwartz, M. D. (2007). Shifting plant phenology in response to global change. *Trends in Ecology & Evolution*, *22*(7), 357–365. https://doi.org/10.1016/j.tree.2007.04.003

Dow, C., Kim, A. Y., D'Orangeville, L., Gonzalez-Akre, E. B., Helcoski, R., Herrmann, V., et al. (2022). Warm springs alter timing but not total growth of temperate deciduous trees. *Nature*, *608*(7923), 1–6. https://doi.org/10.1038/s41586-022-05092-3

Dragoni, D., Schmid, H. P., Wayson, C. A., Potter, H., Grimmond, C. S. B., & Randolph, J. C. (2011). Evidence of increased net ecosystem productivity associated with a longer vegetated season in a deciduous forest in south-central Indiana, USA. *Global Change Biology*, *17*(2), 886–897. https://doi.org/10.1111/j.1365-2486.2010.02281.x

Elliott, K. J., Miniat, C. F., Pederson, N., & Laseter, S. H. (2015). Forest tree growth response to hydroclimate variability in the southern Appalachians. *Global Change Biology*, *21*(12), 4627–4641. https://doi.org/10.1111/gcb.13045

Fu, Y. H., Zhao, H., Piao, S., Peaucelle, M., Peng, S., Zhou, G., et al. (2015). Declining global warming effects on the phenology of spring leaf unfolding. *Nature*, *526*(7571), 104–107. https://doi.org/10.1038/nature15402

Goulden, M. L., Munger, J. W., Fan, S. M., Daube, B. C., & Wofsy, S. C. (1996). Exchange of carbon dioxide by a deciduous forest: Response to interannual climate variability. *Science*, *271*(5255), 1576–1578. https://doi.org/10.1126/science.271.5255.1576

Grossiord, C., Bachofen, C., Gisler, J., Mas, E., Vitasse, Y., & Didion-Gency, M. (2022). Warming may extend tree growing seasons and compensate for reduced carbon uptake during dry periods. *Journal of Ecology*, *110*(7), 1575–1589. https://doi.org/10.1111/1365-2745.13892

Gu, L., Hanson, P. J., Post, W. M., Kaiser, D. P., Yang, B., Nemani, R., et al. (2008). The 2007 eastern US spring freeze: Increased cold damage in a warming world? *BioScience*, *58*(3), 253–262. https://doi.org/10.1641/b580311

Gu, L., Pallardy, S. G., Hosman, K. P., & Sun, Y. (2016). Impacts of precipitation variability on plant species and community water stress in a temperate deciduous forest in the central US. *Agricultural and Forest Meteorology*, *217*, 120–136. https://doi.org/10.1016/j.agrformet.2015.11.014

Gu, L., Pallardy, S. G., Yang, B., Hosman, K. P., Mao, J., Ricciuto, D., et al. (2016). Testing a land model in ecosystem functional space via a comparison of observed and modeled ecosystem flux responses to precipitation regimes and associated stresses in a Central US forest. *Journal of Geophysical Research: Biogeosciences*, *121*(7), 1884–1902. https://doi.org/10.1002/2015jg003302

Helvey, J., & Patric, J. H. (1965). Canopy and litter interception of rainfall by hardwoods of eastern United States. *Water Resources Research*, *1*(2), 193–206. https://doi.org/10.1029/wr001i002p00193

Hollinger, D. Y., Ollinger, S. V., Richardson, A. D., Meyers, T. P., Dail, D. B., Martin, M. E., et al. (2010). Albedo estimates for land surface models and support for a new paradigm based on foliage nitrogen concentration. *Global Change Biology*, *16*(2), 696–710. https://doi.org/10.1111/j.1365-2486.2009.02028.x

Hufkens, K., Friedl, M. A., Keenan, T. F., Sonnentag, O., Bailey, A., O'Keefe, J., & Richardson, A. D. (2012). Ecological impacts of a widespread frost event following early spring leaf-out. *Global Change Biology*, *18*(7), 2365–2377. https://doi.org/10.1111/j.1365-2486.2012.02712.x

Jones, K. (2022). TOS protocol and procedure—PHE—Plant phenology. National Ecological Observatory Network (NEON) Document number NEON.DOC.014040. Retrieved from https://data.neonscience.org/data-products/DP1.10055.001

Kim, J. H., Hwang, T., Yang, Y., Schaaf, C. L., Boose, E., & Munger, J. W. (2018). Warming-induced earlier greenup leads to reduced stream discharge in a temperate mixed forest catchment. *Journal of Geophysical Research: Biogeosciences*, *123*(6), 1960–1975. https://doi.org/10.1029/2018jg004438

Klosterman, S., Hufkens, K., & Richardson, A. D. (2018). Later springs green-up faster: The relation between onset and completion of green-up in deciduous forests of North America. *International Journal of Biometeorology*, *62*(9), 1645–1655. https://doi.org/10.1007/s00484-018-1564-9

Lian, X., Piao, S., Li, L. Z., Li, Y., Huntingford, C., Ciais, P., et al. (2020). Summer soil drying exacerbated by earlier spring greening of northern vegetation. *Science Advances*, *6*(1), eaax0255. https://doi.org/10.1126/sciadv.aax0255

Morin, X., Lechowicz, M. J., Augspurger, C., O'keefe, J., Viner, D., & Chuine, I. (2009). Leaf phenology in 22 North American tree species during the 21st century. *Global Change Biology*, *15*(4), 961–975. https://doi.org/10.1111/j.1365-2486.2008.01735.x

Noormets, A., McNulty, S. G., DeForest, J. L., Sun, G., Li, Q., & Chen, J. (2008). Drought during canopy development has lasting effect on annual carbon balance in a deciduous temperate forest. *New Phytologist*, *179*(3), 818–828. https://doi.org/10.1111/j.1469-8137.2008.02501.x

Novick, K. A., Oishi, A. C., Ward, E. J., Siqueira, M. B., Juang, J. Y., & Stoy, P. C. (2015). On the difference in the net ecosystem exchange of CO 2 between deciduous and evergreen forests in the southeastern United States. *Global Change Biology*, *21*(2), 827–842. https://doi.org/10.1111/gcb.12723

Novick, K. A., Walker, J., Chan, W. S., Schmidt, A., Sobek, C., & Vose, J. M. (2013). Eddy covariance measurements with a new fast-response, enclosed-path analyzer: Spectral characteristics and cross-system comparisons. *Agricultural and Forest Meteorology*, *181*, 17–32. https://doi.org/10.1016/j.agrformet.2013.06.020

Oishi, A. C., Miniat, C. F., Novick, K. A., Brantley, S. T., Vose, J. M., & Walker, J. T. (2018). Warmer temperatures reduce net carbon uptake, but do not affect water use, in a mature southern Appalachian forest. *Agricultural and Forest Meteorology*, *252*, 269–282. https://doi.org/10.1016/j.agrformet.2018.01.011

Oishi, A. C., Novick, K. A., & Stoy, P. (2018). AmeriFlux US-Dk2 Duke Forest-hardwoods, Ver. 4-5 [Dataset]. AmeriFlux AMP. https://doi.org/10.17190/AMF/1246047

Oishi, A. C., Oren, R., Novick, K. A., Palmroth, S., & Katul, G. G. (2010). Interannual invariability of forest evapotranspiration and its consequence to water flow downstream. *Ecosystems*, *13*(3), 421–436. https://doi.org/10.1007/s10021-010-9328-3

Pastorello, G., Trotta, C., Canfora, E., Chu, H., Christianson, D., Cheah, Y. W., et al. (2020). The FLUXNET2015 dataset and the ONEFlux processing pipeline for eddy covariance data. *Scientific Data*, *7*(1), 1–27. https://doi.org/10.1038/s41597-020-0534-3

Pendergrass, A. G., Meehl, G. A., Pulwarty, R., Hobbins, M., Hoell, A., AghaKouchak, A., et al. (2020). Flash droughts present a new challenge for subseasonal-to-seasonal prediction. *Nature Climate Change*, *10*(3), 191–199. https://doi.org/10.1038/s41558-020-0709-0

Peñuelas, J., Rutishauser, T., & Filella, I. (2009). Phenology feedbacks on climate change. *Science*, *324*(5929), 887–888. https://doi.org/10.1126/science.1173004

Piao, S., Friedlingstein, P., Ciais, P., Viovy, N., & Demarty, J. (2007). Growing season extension and its impact on terrestrial carbon cycle in the Northern Hemisphere over the past 2 decades. *Global Biogeochemical Cycles*, *21*(3). https://doi.org/10.1029/2006gb002888

Polgar, C. A., & Primack, R. B. (2011). Leaf-out phenology of temperate woody plants: From trees to ecosystems. *New Phytologist*, *191*(4), 926–941. https://doi.org/10.1111/j.1469-8137.2011.03803.x

Reichstein, M., Falge, E., Baldocchi, D., Papale, D., Aubinet, M., Berbigier, P., et al. (2005). On the separation of net ecosystem exchange into assimilation and ecosystem respiration: Review and improved algorithm. *Global Change Biology*, *11*(9), 1424–1439. https://doi.org/10.1111/j.1365-2486.2005.001002.x

Richardson, A. D., Andy Black, T., Ciais, P., Delbart, N., Friedl, M. A., Gobron, N., et al. (2010). Influence of spring and autumn phenological transitions on forest ecosystem productivity. *Philosophical Transactions of the Royal Society B: Biological Sciences*, *365*(1555), 3227–3246. https://doi.org/10.1098/rstb.2010.0102

Richardson, A. D., Keenan, T. F., Migliavacca, M., Ryu, Y., Sonnentag, O., & Toomey, M. (2013). Climate change, phenology, and phenological control of vegetation feedbacks to the climate system. *Agricultural and Forest Meteorology*, *169*, 156–173. https://doi.org/10.1016/j.agrformet.2012.09.012

Richardson, A. D., & O'Keefe, J. (2009). Phenological differences between understory and overstory. In A. Noormets (Ed.), *Phenology of ecosystem processes*. Springer. https://doi.org/10.1007/978-1-4419-0026-5_4

Roman, D. T., Novick, K. A., Brzostek, E. R., Dragoni, D., Rahman, F., & Phillips, R. P. (2015). The role of isohydric and anisohydric species in determining ecosystem-scale response to severe drought. *Oecologia*, *179*(3), 641–654. https://doi.org/10.1007/s00442-015-3380-9

Schwartz, M. D., & Karl, T. R. (1990). Spring phenology: Nature's experiment to detect the effect of "green-up" on surface maximum temperatures. *Monthly Weather Review*, *118*(4), 883–890. https://doi.org/10.1175/1520-0493(1990)118<0883:spnetd>2.0.co;2

Steinaker, D. F., Wilson, S. D., & Peltzer, D. A. (2010). Asynchronicity in root and shoot phenology in grasses and woody plants. *Global Change Biology*, *16*(8), 2241–2251. https://doi.org/10.1111/j.1365-2486.2009.02065.x

Stoy, P. C., Katul, G. G., Siqueira, M. B., Juang, J. Y., Novick, K. A., McCarthy, H. R., et al. (2008). Role of vegetation in determining carbon sequestration along ecological succession in the southeastern United States. *Global Change Biology*, *14*(6), 1409–1427. https://doi.org/10.1111/j.1365-2486.2008.01587.x

Sulman, B. N., Roman, D. T., Scanlon, T. M., Wang, L., & Novick, K. A. (2016). Comparing methods for partitioning a decade of carbon dioxide and water vapor fluxes in a temperate forest. *Agricultural and Forest Meteorology*, *226*, 229–245. https://doi.org/10.1016/j.agrformet.2016.06.002

Vitasse, Y., Lenz, A., & Körner, C. (2014). The interaction between freezing tolerance and phenology in temperate deciduous trees. *Frontiers in Plant Science*, *5*, 541. https://doi.org/10.3389/fpls.2014.00541

Vitasse, Y., Porté, A. J., Kremer, A., Michalet, R., & Delzon, S. (2009). Responses of canopy duration to temperature changes in four temperate tree species: Relative contributions of spring and autumn leaf phenology. *Oecologia*, *161*(1), 187–198. https://doi.org/10.1007/s00442-009-1363-4

Whitley, R., Medlyn, B., Zeppel, M., Macinnis-Ng, C., & Eamus, D. (2009). Comparing the Penman–Monteith equation and a modified Jarvis–Stewart model with an artificial neural network to estimate stand-scale transpiration and canopy conductance. *Journal of Hydrology*, *373*(1–2), 256–266. https://doi.org/10.1016/j.jhydrol.2009.04.036

Wutzler, T., Lucas-Moffat, A., Migliavacca, M., Knauer, J., Sickel, K., Šigut, L., et al. (2018). Basic and extensible post-processing of eddy covariance flux data with REddyProc. *Biogeosciences*, *15*(16), 5015–5030. https://doi.org/10.5194/bg-15-5015-2018

Yi, K., Dragoni, D., Phillips, R. P., Roman, D. T., & Novick, K. A. (2017). Dynamics of stem water uptake among isohydric and anisohydric species experiencing a severe drought. *Tree Physiology*, *37*(10), 1379–1392. https://doi.org/10.1093/treephys/tpw126

Zohner, C. M., Mo, L., Renner, S. S., Svenning, J. C., Vitasse, Y., Benito, B. M., et al. (2020). Late-spring frost risk between 1959 and 2017 decreased in North America but increased in Europe and Asia. *Proceedings of the National Academy of Sciences*, *117*(22), 12192–12200. https://doi.org/10.1073/pnas.1920816117